

Microscopic mechanism of templated self-assembly: Indium metallic atomic wires on Si(553)-Au

Pil-Gyu Kang, Hojin Jeong, and Han Woong Yeom*

Institute of Physics and Applied Physics and Center for Atomic Wires and Layers, Yonsei University, Seoul 120-749, Korea

(Received 4 February 2009; published 16 March 2009)

We report on the self-assembly of metallic atomic wires utilizing a templated semiconductor surface. A well-ordered template is provided by a vicinal Si surface reacted with Au, Si(553)-Au, which has a regular and robust step array. The scanning tunneling microscopy study shows that In atoms preferentially adsorb and diffuse actively along step edges to form well-ordered atomic wires. The local spectroscopy indicates the metallic property of In atomic wires formed. *Ab initio* calculations reveal the microscopic mechanism of the templated self-assembly as based on well-aligned preferential adsorption sites and the strongly anisotropic surface diffusion. This template can, thus, be widely applied to fabricate various atomic or molecular wires.

DOI: 10.1103/PhysRevB.79.113403

PACS number(s): 68.43.Fg, 68.43.Hn, 68.37.Ef, 73.20.At

Nanoscale or atomic (molecular)-scale structures constitute key elements for various novel devices in nanotechnology and have provided unprecedented material systems to study exotic physics in low dimensions. Among various ways to fabricate nanoscale or atomic-scale structures, the self-assembly on surfaces based on spontaneous interactions among atoms and molecules during the growth on solid substrates has been widely applied to achieve a large-scale growth.¹ However, the self-assembly on surfaces also has crucial limitation in controllable positioning or patterning. Using a prepatterned surface as a template during the self-assembly can obviously be helpful to overcome such limitation for a more sophisticated nanostructure or atomic structure architecture. Various physical or chemical interactions with prepatterned surfaces guide the self-assembly to form arrays of nanoscale or atomic-scale structures as determined by the template patterns. Indeed, a variety of templates has been introduced for self-assembly processes on surfaces such as reconstructed metal^{2,3} or semiconductor⁴ flat surfaces, regular step arrays of vicinal metal⁵ or semiconductor⁶ surfaces, and further molecular adsorbate networks.⁷ However, finding a properly working template is not always easy and straightforward since the microscopic interactions between templates and growing materials are usually intricate and only poorly understood.

Among novel atomic-scale structures, we are particularly interested in metallic atomic wires formed on semiconductor surfaces. Due to the band gap of substrates, these atomic wires have well-isolated electrons, which can form well-defined one-dimensional (1D) metallic bands.⁸⁻¹² Intriguing metal-insulator transitions were observed in In or Au atomic wires formed on Si surfaces due possibly to the Peierls instability^{8,11,13} and more exotic 1D physics, such as non-Fermi-liquid behavior¹⁴ and 1D Rashba effect,¹⁵ have been looked for. These systems were first observed for the self-assembly (or the surface reconstruction) of In or Au adsorbates on the flat Si(111) surface.⁸⁻¹⁰ More recently, a variety of vicinal Si(111) surfaces with more or less regular step arrays¹¹⁻¹³ was utilized to grow Au atomic wires, providing more flexibility in local structures and spacings of wires. However, the success of vicinal Si substrates such as Si(553), Si(557), and Si(5 5 12) is limited and far from the really controllable templated self-assembly since the step morphologies of the substrates (the wire spacing obtained) are usually not preserved and not predictable due to the strong

reconstructive interaction between metals and substrates.^{12,16} This is in contrast to the self-assembly of the atomic wires on metal or inert gas atoms on stepped metal surfaces.^{5,17} Therefore, a more versatile growth method or strategy is requested along with the understanding of the microscopic mechanism underlying the self-assembly of metallic atomic wires on semiconductor surfaces.

In the present work, we succeeded in the fabrication of a well-ordered In atomic-wire array using a vicinal Si(111) surface, Si(553), and explained the microscopic mechanism behind the templated self-assembly. The atomic and electronic structures of the wires were investigated by scanning tunneling microscopy (STM) and scanning tunneling spectroscopy (STS), respectively, and further analyzed by *ab initio* density-functional theory calculations. The deposited In adsorbs and diffuses actively along the step edges to form well-ordered wires with metallic density of states (DOS), where the step structure is stabilized by predeposited Au adatoms. The calculations elucidated the microscopic mechanism of the templated self-assembly as due to the preferential bonding with double dangling-bond (DB) chains along the step edges and the very anisotropic diffusion of adsorbates. The Si(553)-Au template can thus be widely applied to grow various novel atomic wires.

STM/STS experiments were conducted at room temperature (RT) using a commercial microscope (Omicron, Germany). The well-ordered Si(553)-Au surface was prepared by deposition of 0.25 monolayer (ML) Au onto a Si(553) substrate at 930 K (Ref. 13) and then In was deposited at RT by a graphite effusion cell. One monolayer is defined as the density of atoms within the bulk-terminated Si(111) surface layer. The coverages of Au and In evaporated were calibrated by the well-ordered Si(111)5×2-Au and Si(111)4×1-In surfaces with the well-established nominal coverages of 0.4 and 1.0 ML, respectively.^{12,18} The current-imaging tunneling spectroscopy method was utilized, where the feedback control was sequentially on and off for scanning and current-voltage sampling, respectively. Total-energy calculations were performed using the Vienna *ab initio* package¹⁹ with ultrasoft pseudopotentials²⁰ and the generalized-gradient approximation.²¹ The Si(553)-Au surface was modeled by repeated slabs of six Si layers and 12-Å-wide vacuum. We used a 4×1 unit cell by expanding that of bulk-terminated Si(553)1×1 (3.86×14.97 Å² with the short axis along the steps) along the step direction. We used a converging plane-

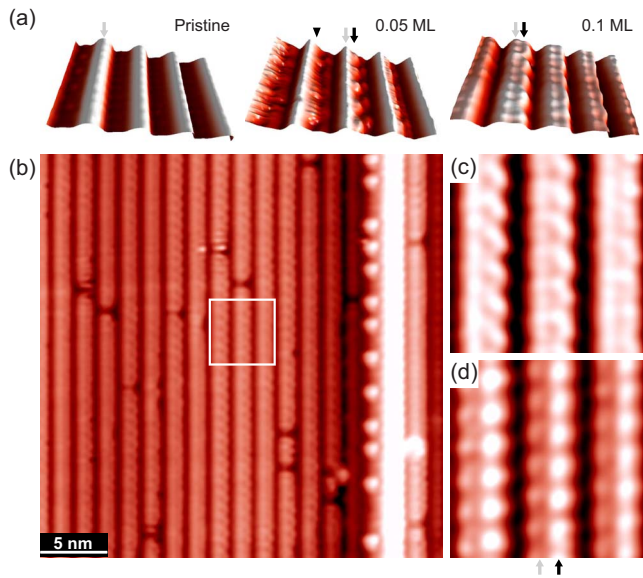


FIG. 1. (Color online) (a) STM topographic images of the pristine Si(553)-Au surface (left) and after depositing onto this surface In of about 0.05 (center) and 0.1 ML (right). Gray and black arrows and an arrowhead indicate Si step-edge chains and rows of bright protrusion and the In-induced flickering stripes, respectively. (b) Large-scale ($30 \times 30 \text{ nm}^2$) STM image after 0.1 ML In deposition and the close-ups of the boxed area in (c) filled (-1.0 V) and (d) empty ($+1.0 \text{ V}$) states. The large surface area consists of two flat regions with regular single-atomic height step arrays, which are separated by a bunched step decorated with Si adatoms (Ref. 20). The tunneling current (I_t) is 50 pA.

wave expansion (15 Ry cutoff energy) and a 2×2 mesh for the momentum-space integration. The STM images were simulated by the Tersoff and Hamann approximation.²²

The Si(553)-Au surface prepared as the template consists mainly of a row of Au atoms substituting terrace Si atoms and a Si step-edge row with the so-called honeycomb chain (HC) reconstruction in each unit cell [dark and bright stripes in the STM image of the left panel in Fig. 1(a), respectively]. Figure 2(a) shows the schematics of a tentative structure model.^{23,24} The deposition of In leads to progressive changes in the surface. As shown in Fig. 1(a), at a much lower coverage than 0.1 ML, we observed the random distribution of the stationary bright protrusions (black arrow) and the “flickering” stripes (arrowhead) adjacent to step-edge rows (gray arrow). When increasing the In coverage, the relative population of the flickering stripes decreases, while that of the bright protrusions increases. As explained below, each bright protrusion is a single stationary In atoms and the flickering stripes are due to diffusing In atoms. When In coverage reaches about $0.1 \pm 0.01 \text{ ML}$, the bright protrusions cover the whole sites adjacent to step edges and form a regular chain array as shown in Figs. 1(a) and 1(b). Beyond 0.1 ML, the chain growth is self-limited and extra In atoms coalesce into islands with various sizes (data are not shown here).

The large-scale STM image [Fig. 1(b)] shows that the saturated In wires are uniform and do not change the step morphology of the substrate. In the detailed filled-state image of Fig. 1(c), the In wires exhibit a $\times 2$ periodicity (0.77 nm) along the wire direction and the interwire distance is

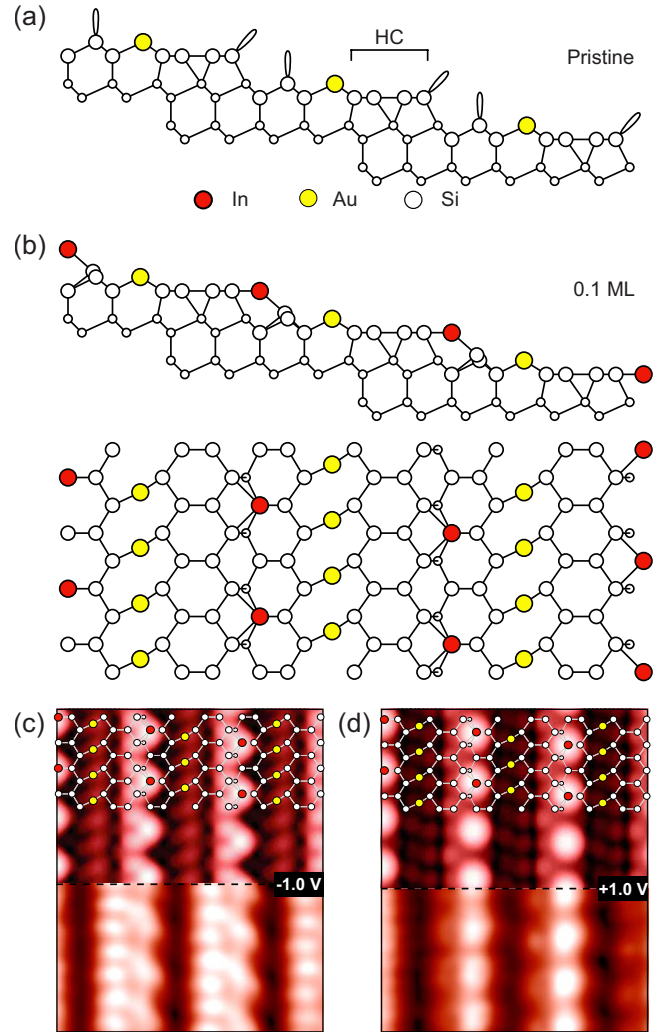


FIG. 2. (Color online) (a) The schematic view of the structure model for the pristine Si(553)-Au surface and (b) for the surface with saturated In atomic wires (0.1 ML). The simulated (top) and topographic (bottom) images for 0.1 ML In at (c) the filled (-1.0 V) and (d) empty ($+1.0 \text{ V}$) states.

1.48 nm as given by the substrate. Note that the step-edge chains also show a rather weak $\times 2$ modulation [clearer in the empty state of Fig. 1(d)] along the steps, which is distinct from the pristine step-edge chains with only a $\times 1$ structure. These surface structures are fully consistent with the well-developed low-energy electron-diffraction (LEED) pattern observed.

In order to understand the changes in the topographic STM images by In deposition, we carried out *ab initio* total-energy calculations. We employed the structure model of the Si(553)-Au surface, proposed by previous works.^{23,24} As mentioned above, this structure [Fig. 2(a)] consists mainly of a Au chain substituting a Si row in the middle of the nanoterrace and a HC structure on the step edge with four Si rows. There are unsaturated DBs on the step-edge Si atom and on one Si terrace atom near the step edge, which form two separated DB chains. We found out that these adjacent DB chains provide ideal adsorption sites for In adatoms. For the single adatom in a 4×1 supercell ($\sim 0.05 \text{ ML}$), the trivalent In adatom is the most stable with the adsorption

energy of 3.44 eV when it makes bonds with two step-edge Si atoms and one terrace Si atom [see Fig. 2(b)]. The bond formation of an In adatom with one step-edge Si atom and two terrace Si atoms, instead, decreases the adsorption energy by 0.10 eV. On the other hand, the adsorption of In atoms on Au chains and HC, where all DB states are presaturated, is highly unstable with their adsorption energies less than that of the most stable structure by 0.27 and 0.65 eV, respectively. At the coverage of 0.10 ML with a 2×1 order shown in Fig. 2(b), three quarters of the surface DBs are saturated. A higher coverage In adsorption makes the system unstable since the calculated energy gain from the bulk In crystal becomes negative due to the unsaturated In valence electrons. This explains the self-limiting behavior of the wire growth at 0.10 ML and the formation of large In islands beyond this coverage.

The saturated 2×1 -In structure at 0.10 ML explains the observed STM images excellently in both filled and empty states as shown in Figs. 2(c) and 2(d). As mentioned above, the major protrusions are due to In adsorbates. Note that the circular and triangular shapes of those protrusions are well reproduced in empty and filled states, respectively. The minor rows of protrusions are due to the Si atomic rows near the step edge. The $\times 2$ modulation appearing along these rows is due to the alternating bonding with In adsorbates on the neighboring step-edge Si row. The energetic consideration and the consistency of the STM images fully support the present structure model of the In atomic wires.

Next, we consider why this Si(553)-Au surface can be a good template for the atomic-wire self-assembly. As shown above, this surface provides the strongly preferential adsorption sites for In atoms by two adjacent DB chains with a proper distance to accommodate the proper In-Si covalent bonds. There are no other possible sites with active DB due to the passivation by Au preadsorption and the HC reconstruction. These DB sites are well aligned along step edges to guide In adsorbates into wires and the growth becomes self-limiting after these sites are consumed. However, these merits are not sufficient and we must also consider the kinetics of adatoms. In order to quantitatively analyze the surface diffusion, we introduced intermediate structures connecting metastable structures and then relaxed them using the nudged elastic band method²⁵ within the *ab initio* total-energy calculation scheme. The pathways and activation energies were obtained by tracing the adatom positions and the energetics of the fully relaxed intermediated structures, respectively. The calculated results displayed in Fig. 3(b) reveal a strong anisotropy in the adatom diffusion. On the pathway parallel to the step edge [the solid line in Fig. 3(a)], the In adatom hops to the next stable site through a metastable position with a small energy barrier of 0.29 eV. This yields an adatom hopping rate along the step edge as high as $\sim 10^9$ Hz at RT if we assume the typical attempt frequency value of $\sim 10^{13}$ Hz.²⁶ On the other hand, the adatom diffuses through two metastable sites across the terrace with a very high barrier of 0.88 eV (a RT hopping rate as low as $\sim 10^{-2}$ Hz). However, the hopping of the adatom from the metastable sites on the terrace (on the Au chain or the HC) into the stable step-edge sites can rather easily take place due to lower activation energies of 0.49 and 0.15 eV, respectively

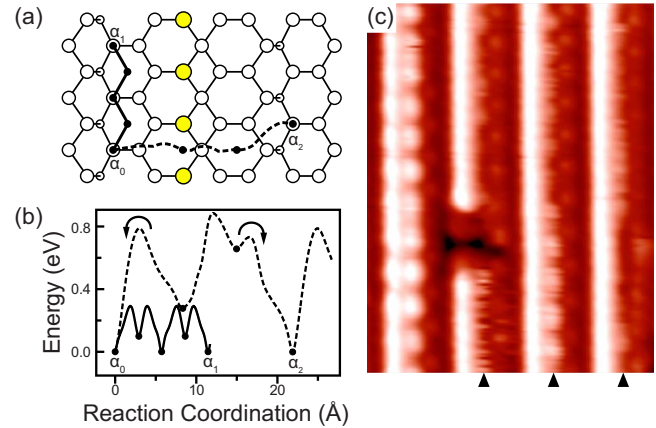


FIG. 3. (Color online) (a) The optimized diffusion paths along (solid) and perpendicular (dashed) to the step direction. (b) The energy variations in the paths along (solid) and perpendicular (dashed) to the step direction given in (a). (c) STM topographic image for the surface with 0.05 ML In. Arrowheads indicate the diffusing In atoms along the step edge appearing as flickering stripes.

[see arrows in Fig. 3(b)]. These results indicate that the adatoms deposited initially on the terrace can rather easily hop into the step-edge sites and diffuse actively only along these sites. Such active 1D diffusion of In atoms was actually observed by STM as the flickering stripes [the arrowheads in Fig. 3(c)], mentioned above, which occur when the step-edge sites are not fully covered below 0.1 ML. The active diffusion at RT also makes it possible to form a well-ordered wire array at relatively low temperature and avoid further reac-

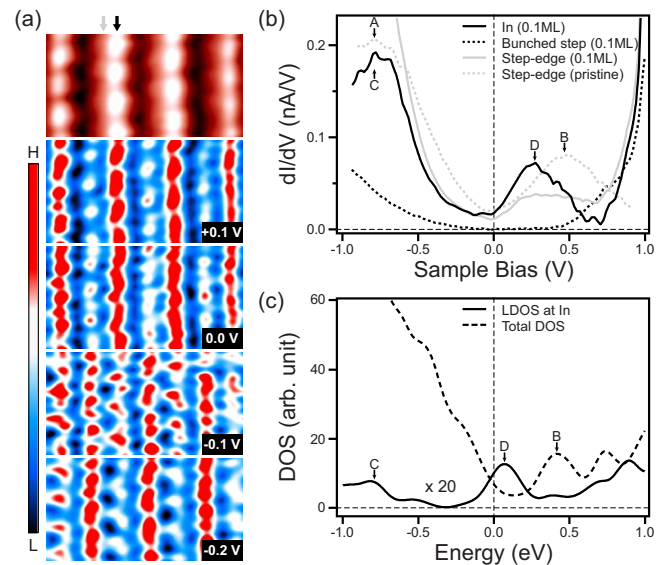


FIG. 4. (Color online) (a) STM topographic image (top) of 0.1 ML In phase (an empty state at +1.0 V) and dI/dV maps (remnants) at the given bias voltages. The scale for the dI/dV intensity, which represents LDOS, is given. (b) Averaged dI/dV spectra on representative sites, including the In chain (black solid), the bunched step (black dashed), the step edge with 0.1 ML In (gray solid), and the pristine step edge (gray dashed). (c) The calculated total DOS of the surface with 0.1 ML In (dashed) and its LDOS projected on the In chain (black solid).

tions at higher temperatures, which destroy the step morphology of the templated substrate.¹⁶

As shown above, the Si(553)-Au surface inherits the well-aligned DB chains and the anisotropic diffusion barriers, which make this surface an ideal template for the growth of atomic wires. This points that various other atoms under proper conditions can self-organize in a similar fashion when they interact with the DBs in a similar way. This can obviously happen for other group-III metals, such as Al and Ga, which show essentially identical adsorption behaviors with In on Si surfaces. We also observed a similar self-organization of atomic wires for a noble-metal Ag on this substrate, which provides promise for the growth of various atomic wires with different electronic, and possibly, magnetic properties.

Finally, we investigated the electronic properties of the In wires by STS as shown in Fig. 4. The dI/dV maps [Fig. 4(a)] near the Fermi level (E_F) reveal dominant local density of state (LDOS) in the empty (filled) states on the In (Au wires). The substantial LDOS at E_F (zero bias) on the In wires indicates their metallic property clearly. Figure 4(b) shows the dI/dV spectra averaged over 20 equivalent positions along the Si row (gray solid line), the In wire (black solid line), and the step-edge chain of the pristine Si(553)-Au surface (gray dashed line). The spectrum of the pristine step-edge chain exhibits two prominent peaks at -0.79 (A) and 0.49 eV (B). A noticeable intensity at E_F indicates the metallic property, in clear contrast to the spectrum (black dashed line) from the insulating part of the surface (the

bunched steps). These spectra are consistent with the previous work.^{13,27} The lack of a strong resonance at E_F in the present system is thought to be due to the fact that the 1D metallic bands of the surface have hole pockets in the center of the Brillouin zone instead of electron pockets. The empty-state peak B is due to the π^* state of the HC along the step edge. On the other hand, the spectrum on the In wire has two peaks, at -0.79 (C) and 0.27 eV (D). Peak D explains the strong empty-state contrast in Fig. 4(a) and its tail explains the metallic LDOS. The C and D peaks are due to the In-Si bonding and antibonding (with a strong p_z character) states, respectively. The partial occupation of the antibonding state D, and thus the metallicity, is thought to be due to the charge transfer from the Au-Si bonding states on the Au chain.

In conclusion, the growth and characteristics of In atomic wires on a templated Si surface, Si(553)-Au, were investigated by STM, STS, and *ab initio* calculations. These studies find the formation of a well-ordered metallic atomic-wire array as properly guided by the Si(553)-Au template with a well-aligned and stabilized step array. The microscopic mechanism of the growth is explained by the local bonding and the highly anisotropic diffusion of adatoms, which make the Si(553)-Au surface a model system to understand the templated self-assembly and promising as a good template for fabricating various atomic-wire arrays.

This work was supported by MOST through Center for Atomic Wires and Layers of the CRi program.

*yeom@yonsei.ac.kr

- ¹J. V. Barth, G. Costantini, and K. Kern, *Nature (London)* **437**, 671 (2005).
- ²M. Böhrringer, K. Morgenstern, W.-D. Schneider, R. Berndt, F. Mauri, A. DeVita, and R. Car, *Phys. Rev. Lett.* **83**, 324 (1999).
- ³T. Classen, G. Fratesi, G. Costantini, S. Fabris, F. L. Stadler, C. Kim, S. D. Gironcoli, S. Baroni, and K. Kern, *Angew. Chem., Int. Ed.* **44**, 6142 (2005).
- ⁴J.-L. Li, J.-F. Jia, X.-J. Liang, X. Liu, J.-Z. Wang, Q.-K. Xue, Z.-Q. Li, J. S. Tse, Z. Zhang, and S. B. Zhang, *Phys. Rev. Lett.* **88**, 066101 (2002).
- ⁵A. Dallmeyer, C. Carbone, W. Eberhardt, C. Pampuch, O. Rader, W. Gudat, P. Gambardella, and K. Kern, *Phys. Rev. B* **61**, R5133 (2000).
- ⁶M. Kawamura, N. Paul, V. Cherepanov, and B. Voigtländer, *Phys. Rev. Lett.* **91**, 096102 (2003).
- ⁷S. Stepanow, M. Lingenfelder, A. Dmitriev, H. Spillmann, E. Delvigne, N. Lin, X. Deng, C. Cai, J. V. Barth, and K. Kern, *Nature Mater.* **3**, 229 (2004).
- ⁸H. W. Yeom, S. Takeda, E. Rotenberg, I. Matsuda, K. Horikoshi, J. Schaefer, C. M. Lee, S. D. Kevan, T. Ohta, T. Nagao, and S. Hasegawa, *Phys. Rev. Lett.* **82**, 4898 (1999).
- ⁹R. Losio, K. N. Altmann, and F. J. Himpsel, *Phys. Rev. Lett.* **85**, 808 (2000).
- ¹⁰W. H. Choi, P. G. Kang, K. D. Ryang, and H. W. Yeom, *Phys. Rev. Lett.* **100**, 126801 (2008).
- ¹¹J. R. Ahn, H. W. Yeom, H. S. Yoon, and I.-W. Lyo, *Phys. Rev. Lett.* **91**, 196403 (2003).
- ¹²J. N. Crain, J. L. McChesney, F. Zheng, M. C. Gallagher, P. C. Snijders, M. Bissen, C. Gundelach, S. C. Erwin, and F. J. Himpsel, *Phys. Rev. B* **69**, 125401 (2004).
- ¹³J. R. Ahn, P. G. Kang, K. D. Ryang, and H. W. Yeom, *Phys. Rev. Lett.* **95**, 196402 (2005).
- ¹⁴P. Segovia, D. Purdie, M. Hengsberger, and Y. Baer, *Nature (London)* **402**, 504 (1999).
- ¹⁵I. Barke, F. Zheng, T. K. Rugheimer, and F. J. Himpsel, *Phys. Rev. Lett.* **97**, 226405 (2006).
- ¹⁶J. R. Ahn, P. G. Kang, J. H. Byun, and H. W. Yeom, *Phys. Rev. B* **77**, 035401 (2008).
- ¹⁷V. Marsico, M. Blanc, K. Kuhnke, and K. Kern, *Phys. Rev. Lett.* **78**, 94 (1997).
- ¹⁸J. Kraft, M. G. Ramsey, and F. P. Netzer, *Phys. Rev. B* **55**, 5384 (1997).
- ¹⁹G. Kresse and J. Hafner, *Phys. Rev. B* **47**, R558 (1993); G. Kresse and J. Furthmüller, *ibid.* **54**, 11169 (1996).
- ²⁰D. Vanderbilt, *Phys. Rev. B* **41**, 7892 (1990).
- ²¹J. P. Perdew and Y. Wang, *Phys. Rev. B* **45**, 13244 (1992).
- ²²J. Tersoff and D. R. Hamann, *Phys. Rev. Lett.* **50**, 1998 (1983).
- ²³K. D. Ryang, P. G. Kang, H. W. Yeom, and S. Jeong, *Phys. Rev. B* **76**, 205325 (2007).
- ²⁴S. Riikonen and D. Sánchez-Portal, *Phys. Rev. B* **77**, 165418 (2008).
- ²⁵G. Mills, H. Jónsson, and G. K. Schenter, *Surf. Sci.* **324**, 305 (1995).
- ²⁶P. G. Kang, H. J. Jeong, and H. W. Yeom, *Phys. Rev. Lett.* **100**, 146103 (2008).
- ²⁷J. N. Crain and D. T. Pierce, *Science* **307**, 703 (2005).